

RESEARCH ARTICLE

Keystone pathobionts associated with colorectal cancer promote oncogenic reprogramming

Josh Jones, Qiaojuan Shi, Rahul R. Nath, Ilana L. Brito *

Meinig School for Biomedical Engineering, Cornell University, Ithaca, NY, United States of America

* ibrto@cornell.edu OPEN ACCESS

Citation: Jones J, Shi Q, Nath RR, Brito IL (2024) Keystone pathobionts associated with colorectal cancer promote oncogenic reprogramming. PLoS ONE 19(2): e0297897. <https://doi.org/10.1371/journal.pone.0297897>

Editor: Syed M. Faisal, University of Michigan Medical School, UNITED STATES

Received: June 7, 2023

Accepted: January 12, 2024

Published: February 16, 2024

Peer Review History: PLOS recognizes the benefits of transparency in the peer review process; therefore, we enable the publication of all of the content of peer review and author responses alongside final, published articles. The editorial history of this article is available here: <https://doi.org/10.1371/journal.pone.0297897>

Copyright: © 2024 Jones et al. This is an open access article distributed under the terms of the [Creative Commons Attribution License](https://creativecommons.org/licenses/by/4.0/), which permits unrestricted use, distribution, and reproduction in any medium, provided the original author and source are credited.

Data Availability Statement: The scRNA-seq data have been deposited in the GEO database (<https://www.ncbi.nlm.nih.gov/geo/>) under accession code GSE220136 (<https://www.ncbi.nlm.nih.gov/geo/query/acc.cgi?acc=GSE220136>).

Abstract

Fusobacterium nucleatum (Fn) and enterotoxigenic *Bacteroides fragilis* (ETBF) are two pathobionts consistently enriched in the gut microbiomes of patients with colorectal cancer (CRC) compared to healthy counterparts and frequently observed for their direct association within tumors. Although several molecular mechanisms have been identified that directly link these organisms to features of CRC in specific cell types, their specific effects on the epithelium and local immune compartment are not well-understood. To fill this gap, we leveraged single-cell RNA sequencing (scRNA-seq) on wildtype mice and mouse model of CRC. We find that Fn and ETBF exacerbate cancer-like transcriptional phenotypes in transit-amplifying and mature enterocytes in a mouse model of CRC. We also observed increased T cells in the pathobiont-exposed mice, but these pathobiont-specific differences observed in wildtype mice were abrogated in the mouse model of CRC. Although there are similarities in the responses provoked by each organism, we find pathobiont-specific effects in Myc-signaling and fatty acid metabolism. These findings support a role for Fn and ETBF in potentiating tumorigenesis via the induction of a cancer stem cell-like transit-amplifying and enterocyte population and the disruption of CTL cytotoxic function.

Introduction

Colorectal cancer (CRC) is caused by both genetic mutations and aberrant features of the gut microbiome. Specifically, two organisms, *Fusobacterium nucleatum* (Fn) and enterotoxigenic *Bacteroides fragilis* (ETBF), are commonly enriched in the gut microbiomes of CRC patients [1–7] and exacerbate intestinal tumor formation in CRC mouse models [5,8]. Although a handful of molecular mechanisms have been identified that directly link these organisms with oncogenic pathways, less is known about how they affect distinct cell types within the intestinal compartment.

Fn was originally identified as an oral pathobiont due to its role in subgingival and periodontal disease [9,10], more recent studies find that Fn is associated with a number of cancers, including esophageal cell carcinoma [11,12], breast cancer [13], and most extensively with CRC [2,7,8,14–17]. Within CRC patients, Fn is spatially enriched in both adenomas and

Funding: This work was supported in part by a grant from the National Cancer Institute (1R33CA235302-01A1). J.J. was funded by a fellowship from the Center for Vertebrate Genomics at Cornell University. I.L.B. was funded by the National Heart, Blood and Lung Institute (1DP2HL141007), a Research Fellowship from the Pew Charitable Trusts and a Fellowship from the David and Lucille Packard Foundation. The funders had no role in study design, data collection and analysis, decision to publish, or preparation of the manuscript.

Competing interests: The authors have declared that no competing interests exist.

adenocarcinomas [7,14,16–18]. Fn is often present on CRC tumor tissue and this is linked to its expression of several adhesins, including FadA [19,20], and Fap2, the latter of which binds to the sugar residue, Gal-GalNAc [21,22], overexpressed on CRC tumors [23]. In addition to these associations, Fn has been shown to play a causative role in neoplastic transformation, with several recognized mechanisms. *Fusobacterium*-specific effector protein Fap2 interacts with TIGIT (T cell immunoreceptor with immunoglobulin and ITIM domain), a potent mediator of immunosuppression, leading to reduced natural killer cell and cytotoxic T cell mediated cytotoxicity [24]. Additionally, in *in vitro* and *in vivo* models of CRC, including the commonly used *Apc*^{Min/+} mouse model, Fn protein FadA has been shown to bind to host cells and promote host DNA damage [25]. This consequently induces beta-catenin and Wnt signaling [26] and annexin A1 expression [27], which together trigger intestinal cell proliferation [8,28].

Under homeostatic conditions, non-toxicogenic *B. fragilis* strains are highly prevalent gut commensals. However, certain *B. fragilis* strains express *B. fragilis* toxin (Bft) and are a common clinicopathological feature in inflammatory bowel disease (IBD) [29–31], diarrheal disease [32], and CRC [3–6]. ETBF has been shown to play a causal role in murine models of CRC. Specifically, Bft acts as a zinc-dependent metalloprotease that degrades E-cadherin, leading to aberrant signaling by beta-catenin and c-myc, both of which support enterocyte growth and proliferation [5,33–36]. Furthermore, ETBF exposure elicits robust pro-tumorigenic IL-17 production and Th17 and T regulatory cell responses [37–40], further establishing a pro-oncogenic role for this pathobiont.

To investigate the effects of Fn and ETBF on host intestinal cells, we exposed a mouse model of CRC, as well as wildtype (WT) mice, to these organisms and performed single-cell RNA sequencing (scRNA-seq) on harvested intestinal resections. We utilized an established CRC mouse model that carries a transversion point mutation in one copy of tumor suppressor, *adenomatous polyposis coli* (*Apc*) (*Apc*^{Min/+}). The biallelic loss of *Apc* is detected in 80–90% of CRC patient cohorts and is an initiating event in sporadic CRC [41–43]. This mutation predisposes the mice to intestinal tumors and has been previously used to study the effects of both Fn and ETBF on tumor initiation and progression [8,15,41–44]. Comparing single-cell transcriptional profiles in resections from both WT and *Apc*^{Min/+} mice afforded the opportunity to disentangle the combined effects of genetics and pathobionts on cellular phenotypes without imposing biases upon which cells these organisms most directly affect.

Results

Fn and ETBF alter intestinal cell composition in *Apc*^{Min/+} and wildtype mice

To determine how CRC pathobionts affect the host intestinal microenvironment, we exposed WT and *Apc*^{Min/+} mice to Fn or ETBF. Mice received a daily oral gavage of Fn or ETBF at a concentration of 10⁸ colony forming units (CFUs) to expose intestinal cells to the pathobionts [8,15,44,45] (Fig 1A). We assessed tumor burden by counting visible tumors upon sacrifice, as described in Kostic *et al.* (2013) [8]. This choice was made due to the presentation of numerous small tumors at 16 weeks. Due to the error in counting tumor volumes for these small tumors, we reasoned that it would be less informative than overall tumor burden. Although Fn and ETBF have been reported to reduce survival rates and increase tumor burdens in *Apc*^{Min/+} mice, these effects were limited to mice pre-treated with antibiotics [8,45–47]. Although antibiotic exposure is associated with increased CRC risk in humans [48–50], we chose not to pre-treat mice with antibiotics to avoid introducing confounding effects on host tissue either directly or via altered microbiome composition. Of note, this experimental procedure does

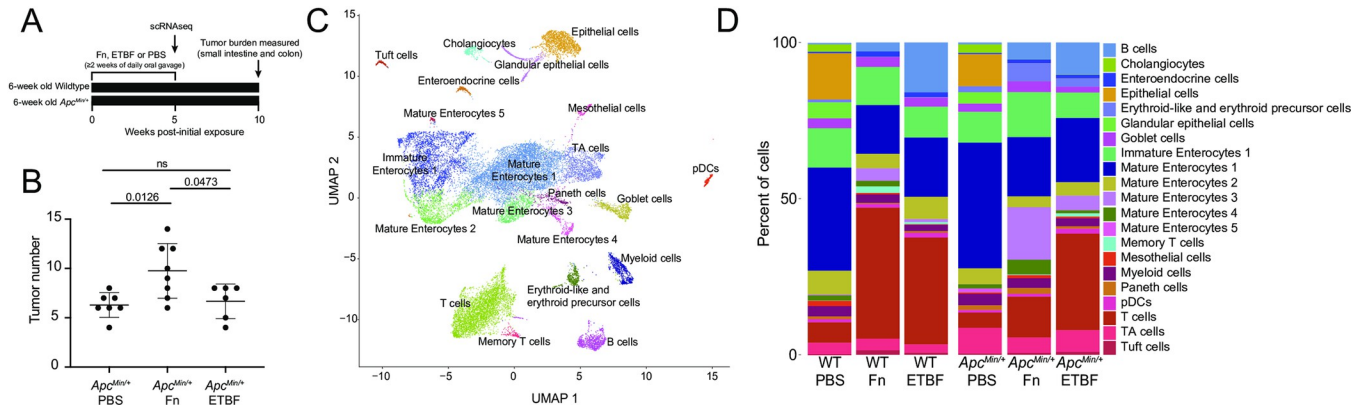


Fig 1. Exposure to CRC-associated pathobionts results in differences in cellular composition and transcriptional profiles. (A) Depiction of the experiment. (B) Macroscopic tumor burden in *Apc^{Min/+}* mice exposed to Fn or ETBF sacrificed at 16 weeks of age ($n \geq 6$ *Apc^{Min/+}* mice). Mice were exposed daily to CRC-associated pathobionts for at least 2 weeks starting at 6-weeks of age. (C) UMAP of transcriptomic profiles of 24,371 cells from all conditions colored according to their annotations. (D) A barplot depicting the composition of cells in each experimental condition.

<https://doi.org/10.1371/journal.pone.0297897.g001>

deviate from established antibiotic-aided colonization methods and may explain why our downstream findings are different from the literature [8,15,44,45]. Nonetheless, we observed greater tumor burden 10-weeks after initial pathobiont exposure in the Fn-exposed *Apc^{Min/+}* mice (Fig 1B), consistent with previous reports [8,51]. We were initially surprised that ETBF administration did not result in increased tumor burden, as it does when ETBF is administered to antibiotic-treated *Apc^{Min/+}* mice [40,44,45]. ETBF administration, under antibiotic treated conditions, elicits a robust IL-17 driven inflammatory response that mediates the recruitment of myeloid cells and ultimately supports tumor cell growth and proliferation in mice [52]. However, contrary to this pro-tumor phenotype, it is also been shown that ETBF does not increase the mutations-per-megabase and copy number alterations above that observed in *Apc^{Min/+}* mice that have been pre-treated with antibiotics [47]. Taken together, without antibiotic-mediated colonization and the resultant inflammation, macroscopic tumor induction post-ETBF exposure was likely tempered.

We performed scRNA-seq on intestinal tissue from WT and *Apc^{Min/+}* mice after oral dosing of Fn or ETBF, or phosphate buffered saline (PBS), as a control. Since Fn and ETBF are enriched in early stages of tumorigenesis (pre-malignant lesions and adenomas) in CRC patients [53–57], we sacrificed mice at 11-weeks of age corresponding to 5 weeks post-pathobiont exposure or PBS treatment. We transcriptionally profiled 24,371 individual cells, which were clustered into 21 different cellular subsets, using Seurat (version 4.1.1) [58]. Cells were annotated with known cell-type specific marker genes [59,60] and cross-referenced using scMRMA, an automated single-cell annotation algorithm [61] (Fig 1C). Cellular compositions across treatment conditions were substantially different, including notable changes across T cells, proliferating enterocyte precursors, and mature enterocytes post-Fn and ETBF exposures (Fig 1D).

Fn and ETBF promote the outgrowth of cancer stem cell-like transit-amplifying cells and cancer-like enterocytes

Transit-amplifying (TA) cells are daughter cells of intestinal stem cells that further differentiate into enterocytes. Due to their high rates of proliferation, they are mutation-prone [62]. Treatment with Fn in co-culture with CRC cell lines has been found to induce the upregulation of stemness associated genes: *CD133*, *CD44*, *Snail1* and *ZEB1* [63,64]. Similarly, ETBF treatment

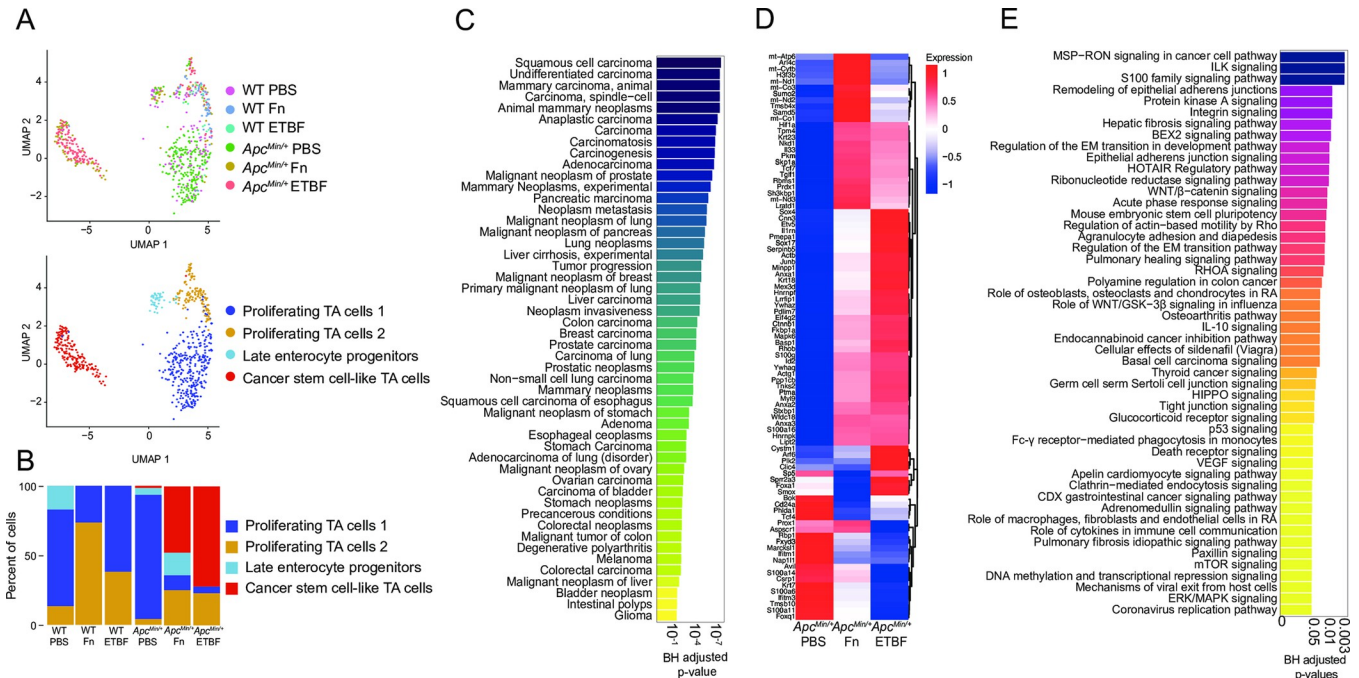


Fig 2. TA cells from *Apc^{Min/+}* mice adopt cancer stem-cell like phenotypes after exposure to CRC-associated pathobionts. (A) UMAP of transcriptomic profiles of TA cells according to experimental condition (top) and subclusters (bottom) (n = 682). (B) A heatmap displaying all 91 upregulated genes for the CSC-like cell cluster (compared to the other TA populations) for each genotype-treatment, ($\log_2(\text{fold-change}) \geq 0.25$ (Wilcox test), Bonferroni-corrected p-value < 0.05, Seurat), plotted as average expression values. (C) A heatmap depicting the top 50 IPA Canonical Pathways genesets for the cancer stem cell-like cell population, based on corrected p-values (BH-FDR-corrected p-value < 0.05, IPA). (D) A barplot depicting the top 50 genesets according to DisGeNET (y-axis) for the CSC-like cell population, plotted in descending according to corrected p-values (Fisher exact test, BH-FDR corrected p-values < 0.05, EnrichR). (E) A barplot depicting the percent composition of the cell populations per genotype and treatment.

<https://doi.org/10.1371/journal.pone.0297897.g002>

leads to the increase in stemness in both CRC cell co-cultures and CRC xenograph mouse models, via the upregulation of *JMJD2B*, a histone demethylase [65]. We hypothesized that exposure to Fn and ETBF in *Apc^{Min/+}* mice would exacerbate neoplastic transformation in these cells accordingly. TA cell transcriptomes sub-clustered into four distinct groups, including one that transcriptionally resembles cancer stem cells (CSCs), based similarities in upregulated genes and pathways between the cells we identified and the known phenotypic profile in the literature [66–69] (Fig 2A–2D). Using DEG analysis, we identified 91 genes delineating these CSC-like cells from the other TA cell subpopulations (Fig 2B). These include upregulated genes that support intestinal cell survival and proliferation, such as *Foxa1* [70–72], *Sox4* [71,73,74], *Prox1* [75–77], and *Ctnnb1* [78–80] (Fisher exact test p-values < 0.05, BH-FDR corrected p-values < 0.05, EnrichR).

This subpopulation was almost exclusively found in the CRC pathobiont-exposed *Apc^{Min/+}* mice (Fig 2E).

Overall, the CSC-like cells upregulated pro-oncogenic pathways, including integrin and integrin-linked kinase (ILK) signaling, MSP-RON (macrophage-stimulating protein-recepteur d’origine nantais) signaling, and Wnt/ β -catenin signaling, among other pathways relating to stem cell pluripotency and the epithelial-mesenchymal transition (EMT) [81–86] (Fig 2C) (Fisher exact test p-values < 0.05, BH-FDR corrected p-values < 0.05, Ingenuity Platform Analysis (IPA) canonical pathway analysis, the gene list used as the input for IPA was the result of a comparison (Wilcoxon test) between CSC-like cell clusters and the other three TA cell clusters). There were few significant differentially enriched pathways between these CSC-like

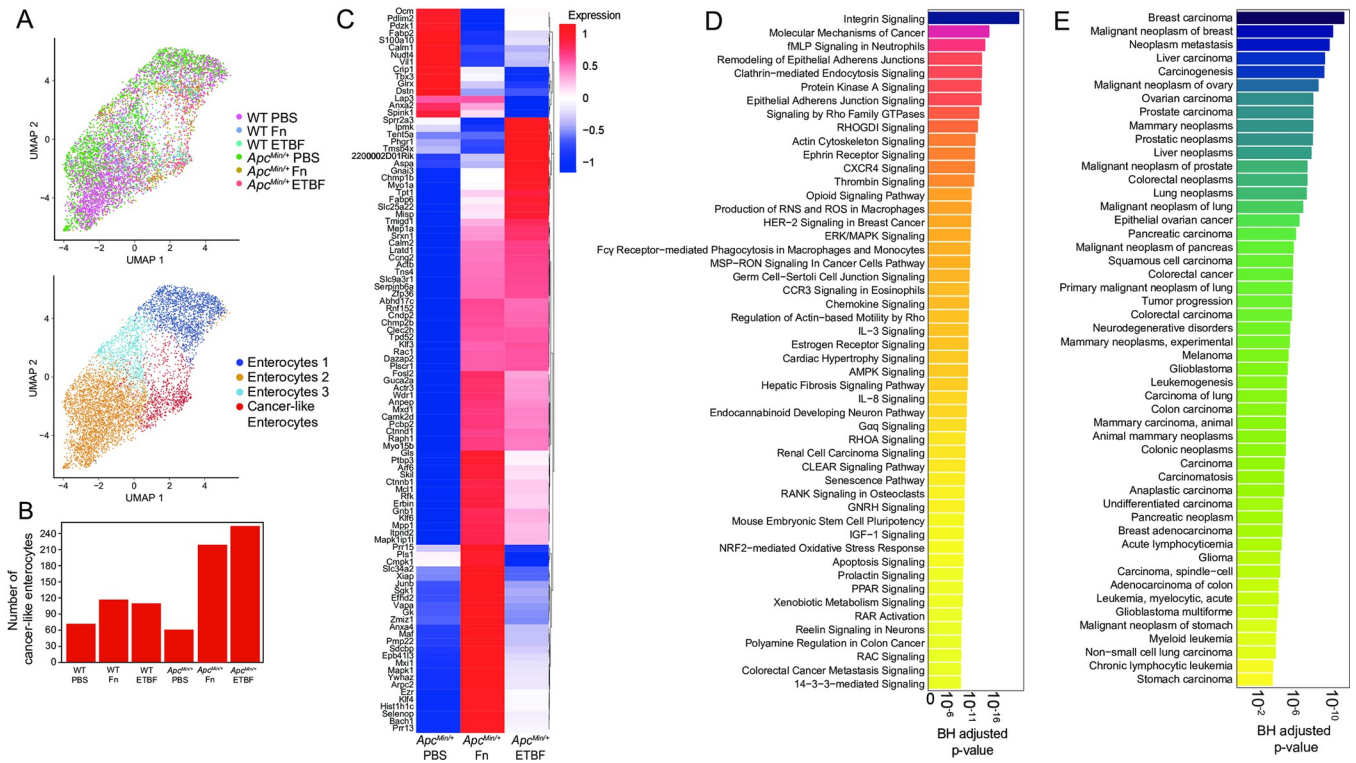
TA cells specific to each pathobiont exposure, although Myc-targeting was comparably elevated in cells derived from *Apc*^{Min/+} mice exposed to ETBF (S1 Fig). As for Fn-exposed CSC-like cell population, fatty acid metabolism was enriched compared to those exposed to ETBF, a finding which is supported by *in vitro* experiments linking this phenotype to enhanced self-renewal (S1 Fig) [63]. The top 50 most significant human gene-disease annotations for the DEGs in the CSC-like TA cell population are all cancers, including several related to the colon (Fig 2D) (Fisher exact test p-values < 0.05, BH-FDR corrected p-values < 0.05, DisGeNET). These colon-specific gene-disease annotations were unique to the CSC-like TA cells (S2 Fig). However, a second cluster of TA cells (proliferating TA cells 2) had similar gene-disease associations to the CSC-like TA cells, albeit different DEGs and enriched pathways. Interestingly, this cluster comprised predominantly cells from wildtype mice exposed to each of the pathobionts (Figs 2E and S3). These data suggest that exposure to CRC-associated pathobionts promotes the induction of cancer-stem cell-like cells within the *Apc*^{Min/+} mice that possess transcriptomic hallmarks of human cancer stem cells.

Mature enterocytes, derived from TA cells, are directly exposed to the microbiome and make up the vast majority of the cells within CRC tumors [68,87]. Both Fn and ETBF treatment increases tumor burden due to the outgrowth of transformed enterocytes in certain mouse models and drive rapid proliferation of epithelial cell lines in co-culture experiments [8,16,26,31,88,89]. Within the mature enterocyte cell population, we performed unsupervised clustering on cellular transcriptional profiles, resulting in four groups (Fig 3A). One group was noticeably enriched for cells derived from *Apc*^{Min/+} mice exposed to Fn and ETBF and displayed a unique cancer-associated profile (Fig 3B and S4). Within this subset, 693 genes are differentially upregulated compared to the other three enterocyte sub-clusters, including the Wnt signaling mediator *Cttnb1*, canonical cancer markers *STAT3* and *HIF1 α* , and *Klf3*, *Klf4*, *Klf5* and *Klf6*, all of which exhibit tumor suppressive properties in many cancers, including CRC [80,90–92] (Figs 3C and S4). When compared to all other mature enterocyte sub-populations, the DEGs for this subset were enriched for genesets involved in PI3K/AKT/mTOR signaling, p53 signaling and apoptotic pathways (Fig 3D) (Fisher exact test p-values < 0.05, BH-FDR corrected p-values < 0.05, EnrichR). Analysis using the IPA platform was consistent with DisGeNET, showing a significant enrichment of disease and functional annotations associated with tumorigenesis (S4 Fig). Overall, these data suggest that this mature enterocyte population from pathobiont-exposed *Apc*^{Min/+} mice adopts a cancer-like phenotype, like that observed in TA cells from the same mice.

Together, these results support a model in which these pathobionts can influence cancer-associated signaling cascades, CRC initiation via CSC-like cell population induction and CRC progression by cancer-like enterocyte enrichment within the context of *Apc*^{Min/+} mouse model. Supporting our work, a recent study investigating the interplay between Fn and human CRC tumors found that epithelial cell population with a high Fn burden upregulated Myc, mTORC1 and PI3K-AKT-mTOR signaling pathways. This important finding suggests that the enrichment of cell growth and proliferation signaling programs are a specific deleterious outcome elicited by Fn and in our study, ETBF as well [7].

Pathobionts elicit similar effects in both-specific effects on cytotoxic T cells are abrogated in *Apc*^{Min/+} mice

T cells are critical for tumor immunosurveillance [93,94]. However, the colorectal tumor microenvironment drives T cells, including potent anti-cancer CD8⁺ cytotoxic T lymphocytes (CTLs), towards immunosuppressive, senescent, and exhaustive states [95–97]. In addition, CRC pathobionts Fn and ETBF exhibit profound T cell modulatory effects. In previous studies



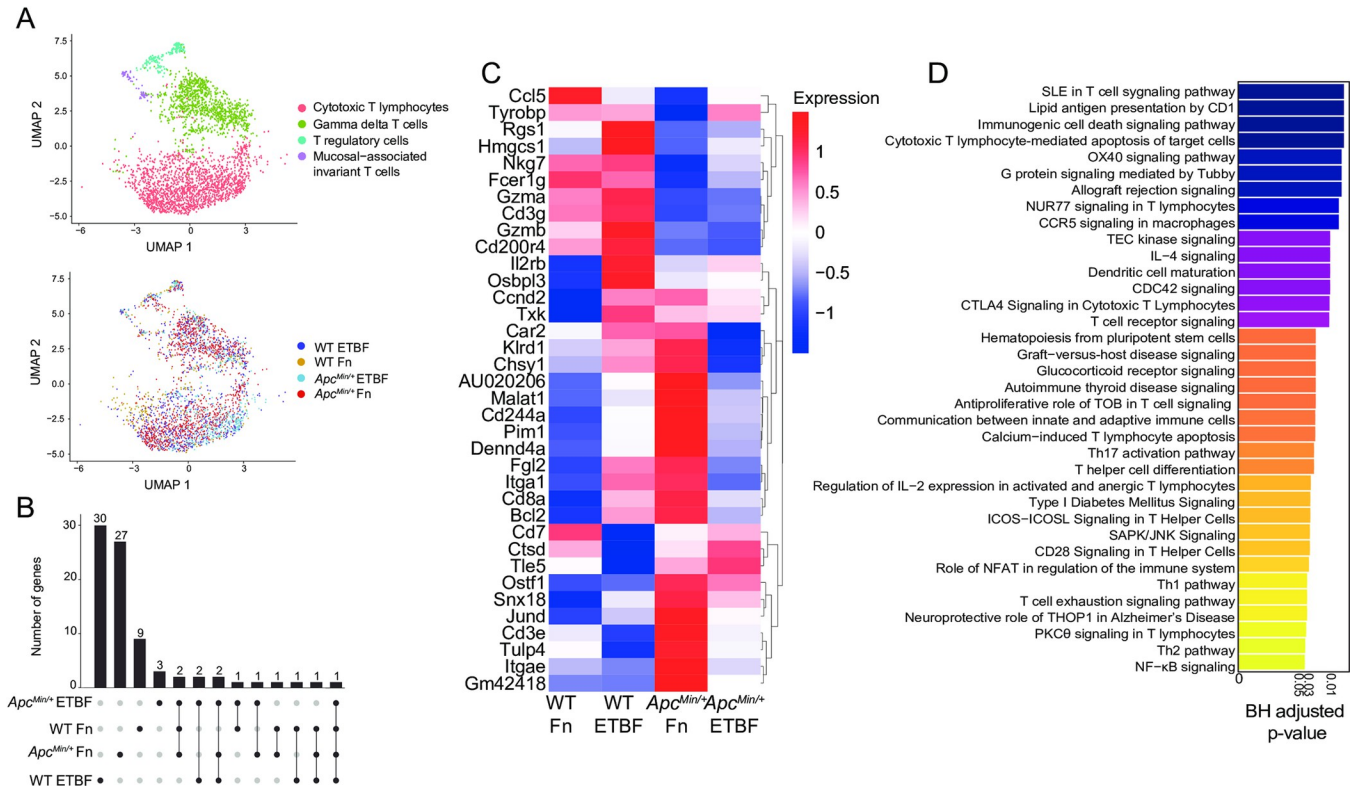


Fig 4. Pathobionts elicit similar effects on cytotoxic T cells are abrogated in *Apc*^{Min/+} mice. (A) UMAP of transcriptomic profiles of 3,101 T cell populations colored by sub-cluster (top) and by experimental condition (bottom). (B) Upset plot depicting the differentially expressed genes that each CTL population ($\log_2(\text{fold-change}) \geq 0.25$, Wilcoxon test, BH-FDR-corrected p-value < 0.05) based on sample, the set size is the total number of genes expressed and the intersection size the number of genes that are shared by dataset, an individual sample alone indicating that the genes are only expressed by the cells in that dataset and lines representing shared genes. (C) A heatmap displaying the top 36 upregulated genes ($\log_2(\text{fold-change}) \geq 0.25$, Wilcoxon test, BH-FDR-corrected p-value < 0.05), plotted as average expression values (Seurat) for the cytotoxic T lymphocytes across each dataset. (D) Barplot depicting the top 36 IPA Canonical Pathways genesets (y-axis) based on corrected p-values (Fisher exact test, BH-FDR corrected p-values < 0.05, IPA). The gene list used as input for canonical pathway analysis were the genes upregulated by ETBF-exposed WT CTLs, when compared to ETBF-exposed *Apc*^{Min/+} CTLs.

<https://doi.org/10.1371/journal.pone.0297897.g004>

numbers of CTLs isolated from the PBS control animals were also low and were therefore removed from downstream analyses. Of the genes that define the CTL cluster, made up of cells from pathobiont-exposed mice, we observed that genes central to CTL function, including the cytolytic granule constituents, *Gzma* and *Gzmb* [101,102], and to a lesser extent *Cxcr6* [103–105], a chemokine receptor, are upregulated in the WT pathobiont-exposed mice, but not the *Apc*^{Min/+} pathobiont-exposed mice (Fig 4B and 4C). These results suggest that the *Apc*^{Min/+} background, possibly due to tumor-mediated immunosuppression, can mollify cytolytic CTL responses that are observed in wild-type post-pathobiont exposed counterparts.

To better understand how the *Apc*^{Min/+} model affects CTLs post-ETBF exposure, we compared the transcriptional profiles from ETBF-exposed *Apc*^{Min/+} with ETBF-exposed WT mice. We found WT ETBF-exposed CTLs upregulated genesets involved in cytotoxic T lymphocyte-mediated apoptosis of target cells, T cell receptor signaling and OX40 signaling pathway [106–108], suggesting that ETBF treatment under normal conditions elicits a robust CTL response, and that this is suppressed in the *Apc*^{Min/+} mice (Fisher’s exact test p-values < 0.05, Bonferroni-corrected p-values < 0.05, IPA canonical pathway analysis) (Fig 4D). These results further support a model where CRC pathobionts induce T-cell dependent immunogenicity that is largely abrogated when tumors are present.

Discussion

Recent cancer pathophysiology studies have shown that the gut microbiota can play a significant role in tumor initiation, progression, or both [109–112]. Within CRC patients' gut microbiomes, organisms such as Fn and ETBF act as pathobionts, because of their ability to induce host inflammation, DNA damage, and cell proliferation [109–111]. These bacteria are thought to initiate the formation of carcinogenic bacterial biofilms and antagonize host immunity by tempering anti-tumor immunity [14,15,24]. Despite a growing body of evidence supporting the role of bacteria in CRC tumor burden and patient survival [109–111], much of the work uncovering the mechanisms underpinning this phenomena have been restricted to experiments using cell culture or on specific cell types isolated from mouse models.

The scRNA-seq data presented here suggests that there are cell-specific and pathobiont-specific effects evident in immune and epithelial tissue. Our analysis reveals that Fn and ETBF can provoke a CSC-like transcriptional profile in TA cells. These CSC-like TA cells bridge pathophysiological observations with specific cellular responses, including, but not limited to, known stemness genes. Moreover, mature enterocytes, which appear to be susceptible to neoplastic transformation, are an emergent feature of *Apc*^{Min/+} intestinal cell profiles post-Fn and ETBF exposure. CTLs, on the other hand, displayed transcriptomes evident of reduced cytotoxic capacity in pathobiont-exposed *Apc*^{Min/+} mice, when compared to their pathobiont-exposed wildtype counterparts. By directly comparing Fn- and ETBF-exposed mice, we observed consistent features invoked by both pathobionts in TA, enterocyte and CTL populations. These results suggest that pathobiont exposure can foster an environment conducive to the outgrowth of tumorigenic intestinal cell populations.

The effects on TA cells, enterocytes and cytotoxic T lymphocytes that we observe were each affected by the underlying genetic background of the CRC mouse model we used. The *Apc*^{Min/+} mouse model recapitulates a relevant mutation in human CRC (80–90% of all sporadic CRC cases) and is therefore the most widely utilized mouse model for CRC. However, there are some notable differences between this model's pathophysiology versus that which is observed in humans. For instance, the primary site of tumorigenesis in the *Apc*^{Min/+} mouse is the small intestine, rather than the colon [113]. Examining the effects of CRC-associated pathobionts in additional mouse models of CRC, including those that exhibit greater colonic tumor burden (e.g. mice carrying inducible mutations in *Apc*, *Kras*, and *p53* specific to the colon, such as those driven by Villin or Cdx2) [114] could further enhance our understanding of colon-specific tumorigenesis mediated by Fn and ETBF. Notwithstanding these alternatives, the *Apc*^{Min/+} model affords the ability to elucidate microbe-specific transcriptional responses in a system free of numerous cancer drivers and in a model within which these organisms have shown to affect tumorigenesis.

This study demonstrates the effects of repeat exposure to CRC pathobionts. There are several limitations of our experimental design. First, we did not use antibiotics nor germ-free mice, as we wanted to maintain the native murine microbiome. This came with the caveat that without antibiotics, Fn and ETBF colonization is not robust. Rather, our results highlight the cellular effects of short-term repeat exposure on intestinal tissue. These results support the hit-and-run carcinogenesis model [115–118], whereby CRC pathobionts exposure is transient but the pro-tumor effects elicited pathobionts manifest by experimental endpoints. Additionally, we were interested in providing a detailed single-cell characterization of both epithelial subtypes and immune cells from both small intestine and colon. For that reason, we pooled and sequenced cells from both anatomical sites. By doing this, we were able to capture epithelial cell heterogeneity, including the detection and characterization of cancer stem cell-like transit-amplifying cells and cancer-like enterocytes. While this method of single-cell preparation

reduced our ability to capture immune cells and other lower abundance cell types such as Paneth and enteroendocrine cells in particular, we avoided examining transcriptional changes induced by cell enrichment methods [119].

Transient exposure, rather than colonization, may have tempered the pro-tumorigenic effects of ETBF (Fig 1B), and possibly Fn, via niche exclusion and/or colonization resistance [120–122]. Moreover, transient exposure and lack of antibiotic use could limit the pathobiont's access to many of the cell populations traditionally associated with their pathogenic inflammatory etiology such T cells and macrophages, which largely are in the lamina propria, and spatial distance from direct interactions with Fn and ETBF, and their pathogen-associated molecular patterns [123,124]. Nonetheless, we still find that transient exposure to Fn and ETBF in the *Apc*^{Min/+} model triggers transcriptional programs that support the outgrowth of CSC-like cells and cancer-like enterocytes. Similar short-term exposures to ETBF induces robust cytotoxic T cell responses in wildtype mice. Taken together, this suggests that Fn and ETBF pro-tumor effects could be more robust than previous thought.

Fn and ETBF are known for their ability to trigger distinct tumor promoting mechanisms. Fn adhesin FadA modulates aberrant Wnt signaling via E-cadherin and β -catenin in enterocytes [26,27]. ETBF possesses a DNA damaging toxin, Bft, and induces Myc signaling in enterocytes and an inflammatory immune cascade largely mediated by Th17 cells and IL-17 [34,35,38]. One of our study's important findings is that Fn and ETBF, despite their unique tumorigenic proclivities, mostly overlap mechanistically as evidenced by the similar cancer-associated transcriptional programs evoked in enterocyte and enterocyte pre-cursors. This suggests that both organisms have common CRC initiating and/or supporting characteristics that affect similar cell types. These findings were enabled by the significant number of enterocytes sequenced across our murine intestinal samples. Herein lies a key shortcoming as well, which does not represent common biology. By probing thousands of enterocytes, other rarer cell types were found in smaller numbers. For this reason, comparative analyses between Fn and ETBF treatments across almost all other cell types, including across both *Apc*^{Min/+} and wild-type mice, were underpowered, and we could not delineate statistically significant differences (BH corrected p-value < 0.05). Nevertheless, our findings still represent an important step in delineating enterocyte and TA cell-specific transcriptomic changes post CRC pathobiont exposure and warrants future investigations delving into larger swath of intestinal cells in depth.

Although Fn and ETBF are perhaps the most well-known CRC-associated pathobionts, a fuller picture of CRC initiation and progression likely involves other key microbial players. For example, *pks*⁺ *E. coli* is an *E. coli* strain that produces colibactin, a genotoxin that cause double strand breaks in the intestinal cells' DNA also has the ability to transform cells [125–127]. The development of polymicrobial biofilms is another emergent feature of CRC. Biofilms are significantly enriched in right sided colon adenomas (precancerous lesion) versus adjacent healthy tissue and have been causally linked with CRC in mouse models [14,15,128]. Additionally, other oral pathobionts beyond Fn, such as *Parvimonas micra*, *Peptostreptococcus stomatis*, *Peptostreptococcus anaerobius* and *Gemella morbillorum*, are commonly enriched in patients with CRC [111,129,130]. Experimentally, *P. anaerobius* and *P. micra* having been shown to play a causal role in oncogenesis in azoxymethane and *Apc*^{Min/+} mouse models, respectively [131,132]. Pertaining to these organisms, major questions in the field remained about how these oral microbes, in concert with gut pathobionts, seed biofilms and, if so, whether the biofilms promote tumorigenesis in the colon [126,133–136]. Performing similarly designed scRNA-seq experiments using additional organisms and eventually consortia will likely be invaluable in delineating the modulatory effects gut bacteria have on CRC tumor initiation and development.

Tumor-specific microbiomes, biofilm formation, and microbiome dysbiosis are all implicated in CRC progression. Using scRNA-seq, we were able to reconstruct cell type-specific effects that occur post-pathobiont exposure. However, recently developed approaches that enable combined host transcriptomics with microbiome species mapping [137,138] will provide additional spatial contextualization, directly associating specific gut microbiota with cell-specific transcriptional changes occurring within the tumor microenvironment. Studying the effects of Fn, ETBF and other pathobionts *in vivo*, using unbiased approaches like these offer the promise of identifying marker genes that may be used to enhance cancer diagnostics and therapeutics.

Materials and methods

Ethical considerations

This study conformed to the National Institutes of Health guidelines on the care and use of laboratory animals. Mouse studies were performed following procedures approved by the Institutional Animal Care and Use Committee at Cornell University (Protocol ID #2016–0088). Mice were monitored daily by staff at the Center for Animal Resources and Education (CARE) and sacrificed either at the end of the study or at ethical endpoints: any indication of poor health including but not limited to the following: decreased activity, dehydration, abnormal fur changes, ataxia, and/or excess weight loss (20% loss of total body weight). Any distress would result in a notification and mice were provided with heat pads and wet chow. Additional water was provided in closer proximity to the ground. Any type of leak in the water was remedied the same day, with dry caging and bedding provided. All researchers handling mice received training through CARE. Due to the nature of the mouse model used in these experiments, in which numerous small (visible) tumors are formed, we chose to assess tumor burden rather than tumor volume, which is more commonly used for xenograft tumor experiments.

Bacterial strains and culturing

Fusobacterium nucleatum subsp. *nucleatum* strain VPI 4355 [1612A] (ATCC 25586) was purchased from American Type Culture Collection (ATCC). *Bacteroides fragilis* (Veillon and Zuber) Castellani and Chalmers strain 2-078382-3 (ATCC 43858) (ETBF) was purchased from American Type Culture Collection (ATCC). Fn and ETBF were grown anaerobically at 37°C on Bacto™ Brain Heart Infusion Broth (BD, Sparks, MD) supplemented with 0.01% Hemin in 1M NaOH, 0.1% Resazurin (25 mg/100ml distilled water), 10% NaHCO₃ in distilled water, and agar if bacteria were plated. Bacteria were grown overnight and diluted to 10⁸ colony forming units (CFU), the amount needed for oral gavage.

Mice

All mice (C57BL/6-*Apc*^{Min/+}/J and C57BL/6-Wild type) were maintained at the barrier mouse facility at Weill Hall at Cornell University. *Apc*^{Min/+} and wild-type mice were initially ordered from Jackson Laboratory and then bred in the barrier facility. The *Apc*^{Min/+} mice used in these experiments have a chemically induced transversion point mutation (a T to an A) at nucleotide 2549. This results in a stop codon at codon 850, truncating the APC protein. Both male and female mice were used in all experiments. Experimental and breeding mice were provided with *ad libitum* access to autoclaved water and rodent chow (autoclavable Teklad global 14% protein rodent maintenance diet #2014-S; Envigo). To avoid cage effects on the microbiota, mice were housed individually at the time of initial Fn, ETBF or PBS exposure. One mouse per condition (6 mice total) were used for the scRNA-seq experiments, whereas ten mice started

the tumor burden study. To monitor for infectious agents such as helminths, sentinel mice were used during the duration of the experiment in the mouse facility to ensure that results following perturbation with Fn and ETBF were a result of specific bacteria and not confounding agents. Every week, food intake and animal weight were recorded, and mice were placed in clean cages with freshly autoclaved chow and water weekly. Food intake and weight was recorded to ensure that mouse tumor burden did not violate ethical standards. Mice were handled under inside a biosafety cabinet with frequent glove changes and disinfection between mice during stool collection and monitoring of body weight. Stool was collected weekly throughout the course of all experiments. Bacterial oral gavage experiments were performed every day for a period of at least 14 consecutive days for ETBF, and up 35 days for Fn [8,25,45], beginning at 6 weeks of age. Bacteria were fed at a concentration of 10^8 CFU per day. Sham treatment consisted of sterile Ca^{2+} and Mg^{2+} free phosphate buffered saline gavaged daily for the entirety of the experiment. Single-cell RNA experiments concluded when the mice were 11 weeks old and tumor burden experiments concluded when mice were 16 weeks old. Several mice in the tumor burden study reached humane endpoints prior to 16 weeks and were not used in assessing tumor burden (3, 2 and 4 mice in the PBS, Fn and ETBF $Apc^{Min/+}$ groups respectively). Mice of both sexes were used for all experiments and were monitored daily. Mice were sacrificed using 5 minutes of CO_2 asphyxiation either at the end of the study or when they reached humane endpoints (see above).

Tumor burden enumeration

For tumor enumeration, $Apc^{Min/+}$ mice were euthanized at 16 weeks of age, and colons and small intestines were excised. Macroscopic (visible) tumors were counted from both anatomical sites, as established previously in Kostic *et al.* (2013) [8]. This model differs from xenograft experiments in which tumor burden is often measured. Due to the numerous small tumors formed in the $Apc^{Min/+}$ mouse model, tumor volume could not be calculated accurately; we therefore relied on tumor enumeration. Tumor counts were plotted using Prism (version 8.2.1). For statistical analysis, Mann-Whitney two-tailed tests were used to compare treatment groups using Prism. Each groups had an $n \geq 6$ mice.

Single cell dissociation from fresh mouse colons and small intestines

This protocol was adapted from Haber *et al* 2017 [59]. To generate single-cell suspensions, $Apc^{Min/+}$ and wild type mice were euthanized at 11 weeks of age, colons and small intestines were excised, rinsed with ice cold sterile 1X Ca^{2+} and Mg^{2+} free PBS (Gibco, 14190144) and flushed of fecal contents using a blunt 1.5-inch 22G needle filled with ice cold sterile 1X Ca^{2+} and Mg^{2+} free PBS (Gibco, 14190144). The tissue was opened longitudinally and sliced into small fragments roughly 1 cm in length. The tissue was incubated in RPMI supplemented with L-glutamine (Corning, 45000–396), 1 mM EDTA (Neta Scientific, QB-A611-E177-10), and 10% FBS (Avantor, 97068–085) for 90 minutes, shaking every 30 minutes. The tissue was then incubated at 37°C for 15 minutes and continuously shaken. The supernatant was passed through a 100 μm cell strainer and held on ice until loading the cells on 10X Chromium. The remaining tissue was resuspended in RPMI (Corning, 45000–396) supplemented with 20% FBS (Avantor, 97068–085), 0.1 mg/ml DNase I (Thermo Scientific, 90083), and 0.5 mg/ml collagenase A (Millipore Sigma, 10103586001) and incubated at 37°C on a shaker for 30 minutes. The tissue was then gently mechanically dissociated using a rubber plunger of a syringe. The tissue and the dissociated contents were passed through a 100 μm cell strainer. The single cell suspension was then pelleted via centrifugation (400 x g for 10 minutes at 4°C). The cell suspension was resuspended in 1X Ca^{2+} and Mg^{2+} free PBS (Gibco, 14190144) containing 0.04%

weight/volume BSA (VWR, 97061–420) and combined with earlier collected fraction and placed on ice. Sample viability was determined before loading the cells on 10X Chromium using the Countess II Automated Cell Counter (ThermoFisher). The desired number of transcripts from viable cells for each sample was 5000–6000 cells per sample.

Single-cell RNA sequencing library preparation

5000–6000 viable ($\geq 70\%$ alive) cells per sample (from colon and small intestine tissues) were targeted on the 10X Genomics Controller using one lane per mouse/sample for Gel Beads in Emulsion (GEM). Cells from the small intestine and colon were pooled together before GEM creation. Briefly, cells were separated into GEMs along with beads coated in oligos that capture mRNAs using a poly-dT sequences. This was followed by cell lysis and barcoded reverse transcription of mRNA, followed by amplification, and enzymatic fragmentation and 5' adaptor and sample index attachment. Single-cell libraries were generated using the Chromium Next GEM Single Cell 3' Library Construction V3 Kit (10X Genomics) and were then sequenced on an Illumina NextSeq 2000 run with the 100 bp P2 kit for all samples. Sequencing data were aligned to the mouse reference, mm10 (Ensembl 84) reference genome using the Cell Ranger 5.0.1 pipeline (10X Genomics).

Single-cell RNAseq data processing and visualization

The output of Cell Ranger is a cell-by-gene unique molecular identifier (UMI) expression matrix for each sample. The expression matrices for each sample are loaded into the Seurat R package (Seurat version 4.1.1, R version 4.1.0 and 4.2.0). The standard Seurat dataset processing workflow was followed. In brief, cells with less than 200 genes, more than 2,500 genes, and more than 35% mitochondrial genes are filtered out. After filtering, the remaining cells were normalized by the total expression, multiplied by the default scale factor (10,000), and log transformed. We then used default Seurat functions to identify highly variable genes with one parameter modification. FindVariableFeatures' nfeature parameter was set to 3,000 instead of 2,000 (default). Next, we scaled the data to regress out variation from mitochondrial genes. We performed principal component analysis (PCA) on the scaled data with variable genes. The top 20 principal components were used for downstream analysis, including dimensionality reduction steps including clustering cells to identify cell populations (clusters). We implemented Uniform Manifold Approximation and Projection for dimensional reduction using the top 20 PCs and visualized.

Marker-gene identification and cell-type annotation

To define cell types for each cluster, we used Seurat's FindAllMarkers with the following parameters: a minimum percent expression value of 25%, \log_2 fold change threshold of 0.25 and a corrected p-value < 0.05 (Bonferroni correction). We looked only at transcripts that were upregulated. We analyzed canonical markers and assigned cell annotations accordingly. We cross-referenced our cell type annotations with gene lists defined in Haber et al. [59] and Moor et al. [60] We cross-reference the cell type assignments with a single cell annotation algorithm, scMRMA in R as well [61].

Reclustering, visualization, and analysis of transit-amplifying cells, mature enterocyte (1) and T cell populations

We used the 682 TA cells, 6,719 mature enterocytes (1), and 3,101 T cells and re-clustered them using Seurat. Marker genes for each subclusters were identified using a minimum

percent expression value of 25%, \log_2 fold change threshold of 0.25 and a corrected p-value < 0.05 (Bonferroni correction) in Seurat. Cell types were assigned based on the expression of these marker genes. Cell clusters expressing marker genes from multiple unrelated cell types (doublets) were removed from analysis. All sub-clustering analysis was carried out with 20 principal components and similar resolution parameters; TA cells and T cells were analyzed with a resolution of 0.4 and mature enterocytes (1) with a resolution of 0.3 in Seurat. The marker gene list used to classify cell subtypes can be found in [S1 Table](#). Cell populations were visualized using Uniform Manifold Approximation and Projection in Seurat. Cell were enumerated, whether as percent of sample or absolute count, using the dittoSeq's (version 1.8.1) bar plot visualization function.

Differential gene expression and geneset enrichment analysis

Differentially gene expression was carried out using Seurat's FindAllMarkers and FindMarkers functions with the following cutoffs: $\log_2(\text{fold change}) \geq 0.25$ (Wilcox test), corrected p-value < 0.05 (Bonferroni correction) and a minimum percent expression value of either the default, 10%, or 25% for certain other analyses. For these analyses, only upregulated genes were used. We visualized DEGs using the Seurat's DoHeatmap and dittoHeatmap (dittoSeq) for heatmaps, dittoPlot(dittoSeq) for violin plots and UpSetR (version 1.4.0) for upset plots. For statistics associated with violin plots ([S4 Fig](#)), we performed a two-sample Wilcoxon test, comparing each normal enterocyte cluster against the cancer-like enterocyte cluster using the `stat_compare_means` function in `ggpubr` (version 0.5.0). For gene set enrichment analysis, the gene list used as input were generated as detailed above using FindMarkers (Seurat). A suite of tools and databases were implement for these analysis and are as follows: Ingenuity Pathway Analysis (IPA, Qiagen) including canonical pathway and disease and function analysis, DisGeNET (version 7.0) via Enrichr [[139,140](#)], and MSigDB Hallmarks 2020 via EnrichR [[140](#)].

Supporting information

S1 Fig. CSC-like TA cells from Fn- and ETBF-exposed *Apc*^{Min/+} mice differed in key pathways. (A) Top 20 differentially enriched pathways (MSigDB Hallmarks 2020) represented in the transcriptomes of cells from CSC-like TA cells from the Fn-exposed *Apc*^{Min/+} mouse as compared to the PBS-treated *Apc*^{Min/+} mouse. (n = 175 cells, Fisher exact test, BH-FDR-corrected p-values < 0.05 , EnrichR) (B) Top 3 differentially enriched pathways (MSigDB Hallmarks 2020) represented in the transcriptomes of cells from CSC-like TA cells from the ETBF-exposed *Apc*^{Min/+} mouse as compared to the PBS-treated *Apc*^{Min/+} mouse. (n = 175 cells, Fisher exact test, BH-FDR-corrected p-values < 0.05 , EnrichR). [S1 Fig](#) complements [Fig 2](#). (TIF)

S2 Fig. Cancer-specific gene-disease associations with DEGs identified in TA cells were specific to those from pathobiont-exposed *Apc*^{Min/+} mice. (A) A barplot depicting the top 50 genesets according to DisGeNET (y-axis) for the proliferating TA cells (1), plotted in descending according to corrected p-values (x-axis, Fisher exact test, BH-FDR corrected p-values < 0.05 , EnrichR). (B) A barplot depicting the top 50 genesets according to DisGeNET (y-axis) for the proliferating TA cells (2), plotted in descending according to corrected p-values (Fisher exact test, BH-FDR-corrected p-values < 0.05 , EnrichR). (C) A barplot depicting the top 14 genesets according to DisGeNET (y-axis) for the late enterocyte progenitors, plotted in descending according to corrected p-values (Fisher exact test, BH-FDR corrected p-values < 0.05 , EnrichR). [S2 Fig](#) complements [Fig 2](#). (TIF)

S3 Fig. Proliferating TA cells 2, similar to CSC-like TA cells in notable disease associations, diverge at the gene and pathway levels. (A) The TA cells depicted here are the 4 subclusters of the complete TA cell population and are an aggregate from all mouse samples ($Apc^{Min/+}$ mice treated with PBS, Fn or ETBF and wild type mice treated with PBS, Fn or ETBF). A heatmap displaying the top 20 upregulated genes for each TA cluster, $\log_2(\text{fold-change}) \geq 0.25$ (Wilcox test), corrected p-value < 0.05 (Bonferroni correction), Seurat, plotted as average expression values (Seurat). (B) Differentially enriched pathways represented in the transcriptomes of proliferating TA cells 2 compared with other TA cell populations. Barplot depicting the top 10 genesets according to the Molecular Signatures Database Hallmark 2020 (MSigDB Hallmarks 2020) for the cancer-like cell population, plotted in descending according to corrected p-values (Fisher exact test, BH-FDR corrected p-values < 0.05 , EnrichR). **S3 Fig** complements **Fig 2** and **S2 Fig**.

(TIF)

S4 Fig. Transcriptome profiles of cancer-like enterocytes were enriched in cancer-like genes and pathways. (A) Violin plots displaying selected CRC-associated genes and their expression levels across 4 enterocyte clusters ($\log_2(\text{fold-change}) \geq 0.25$, Wilcoxon test, Bonferroni-corrected p-value < 0.05). (B) Barplot depicting the top 50 IPA Diseases and Functions annotations based on corrected p-values (Fisher exact test, BH-FDR corrected p-values < 0.05 .) for the cancer-like enterocyte subpopulation. Statistical comparisons were performed using a pairwise Wilcoxon test (* = $p \leq 0.05$, ** = $p \leq 0.01$, *** = $p \leq 0.001$, **** = $p \leq 0.0001$), comparing the cancer-like enterocyte population to all other mature enterocyte clusters (see **S4 Fig**). **S4 Fig** complements **Fig 3**.

(TIF)

S5 Fig. Proinflammatory macrophages derived from the Fn-exposed $Apc^{Min/+}$ mouse upregulate pathways associated with TGF- β /SMAD signaling and epithelial-to-mesenchymal transition. (A) A heatmap displaying the top 50 upregulated genes defining the proinflammatory macrophage population compared across each dataset ($\log_2(\text{fold-change}) \geq 0.25$, Wilcoxon Rank Sum test, p-value < 0.05 (unadjusted), Seurat), plotted as average expression values. (B) Barplot depicting the top 50 enriched genesets according to the Gene Ontology Biological Processes 2021 (GOBP21) for proinflammatory macrophages derived from Fn-exposed $Apc^{Min/+}$ mice when compared to PBS control $Apc^{Min/+}$ mice, plotted in descending according to p-values (Fisher exact test p-values < 0.05 , unadjusted, EnrichR). (C) Barplot depicting the top 50 enriched genesets according to the Gene Ontology Biological Processes 2021 (GOBP21) for proinflammatory macrophages derived from Fn-exposed $Apc^{Min/+}$ mice when compared to ETBF exposed $Apc^{Min/+}$ mice, plotted in descending according to p-values (Fisher exact test p-values < 0.05 , unadjusted, EnrichR).

(TIF)

S1 Table. Genes used to classify single cells. The top 10 differentially expressed genes per cluster listed were used to classify single-cells into cell types. Marker genes were defined using the FindAllMarkers function in Seurat ($\log_2(\text{fold-change}) \geq 0.25$ (Wilcox test), corrected p-value < 0.05 (Bonferroni correction)). The top 10 marker genes were included for each cluster.

(DOCX)

Acknowledgments

We thank the de Vlaminck lab for helpful conversations and feedback.

Author Contributions

Conceptualization: Josh Jones, Ilana L. Brito.

Data curation: Josh Jones.

Formal analysis: Josh Jones, Rahul R. Nath.

Funding acquisition: Ilana L. Brito.

Investigation: Josh Jones, Qiaojuan Shi, Ilana L. Brito.

Methodology: Josh Jones, Qiaojuan Shi, Ilana L. Brito.

Project administration: Qiaojuan Shi, Ilana L. Brito.

Supervision: Qiaojuan Shi, Ilana L. Brito.

Validation: Josh Jones.

Visualization: Josh Jones, Rahul R. Nath.

Writing – original draft: Josh Jones, Ilana L. Brito.

Writing – review & editing: Josh Jones, Qiaojuan Shi, Ilana L. Brito.

References

1. Kostic AD, Gevers D, Pedamallu CS, Michaud M, Duke F, Earl AM, et al. Genomic analysis identifies association of *Fusobacterium* with colorectal carcinoma. *Genome Res* 2012; 22:292–8. <https://doi.org/10.1101/gr.126573.111> PMID: 22009990
2. Castellarin M, Warren RL, J. Douglas Freeman, Freeman JD, Freeman JD, Dreolini L, et al. *Fusobacterium nucleatum* infection is prevalent in human colorectal carcinoma. *Genome Research* 2012; 22:299–306. <https://doi.org/10.1101/gr.126516.111> PMID: 22009989
3. Viljoen KS, Dakshinamurthy A, Goldberg P, Blackburn JM. Quantitative profiling of colorectal cancer-associated bacteria reveals associations between *Fusobacterium* spp., enterotoxigenic *Bacteroides fragilis* (ETBF) and clinicopathological features of colorectal cancer. *PLoS ONE* 2015; 10:1–21. <https://doi.org/10.1371/journal.pone.0119462> PMID: 25751261
4. Boleij A, Hechenbleikner EM, Goodwin AC, Badani R, Stein EM, Lazarev MG, et al. The *Bacteroides fragilis* toxin gene is prevalent in the colon mucosa of colorectal cancer patients. *Clinical Infectious Diseases* 2015; 60:208–15. <https://doi.org/10.1093/cid/ciu787> PMID: 25305284
5. Haghi F, Goli E, Mirzaei B, Zeighami H. The association between fecal enterotoxigenic *B. fragilis* with colorectal cancer. *BMC Cancer* 2019; 19:879. <https://doi.org/10.1186/s12885-019-6115-1> PMID: 31488085
6. Jasemi S, Emaneini M, Fazeli MS, Ahmadinejad Z, Nomanpour B, Sadeghpour Heravi F, et al. Toxigenic and non-toxigenic patterns I, II and III and biofilm-forming ability in *Bacteroides fragilis* strains isolated from patients diagnosed with colorectal cancer. *Gut Pathogens* 2020; 12:1–7. <https://doi.org/10.1186/s13099-020-00366-5>.
7. Niño JLG, Wu H, LaCourse KD, Kempchinsky AG, Baryames A, Barber B, et al. Effect of the intratumoral microbiota on spatial and cellular heterogeneity in cancer. *Nature* 2022:1–8. <https://doi.org/10.1038/s41586-022-05435-0>.
8. Kostic AD, Chun E, Robertson L, Glickman JN, Gallini CA, Michaud M, et al. *Fusobacterium nucleatum* Potentiates Intestinal Tumorigenesis and Modulates the Tumor-Immune Microenvironment. *Cell Host & Microbe* 2013; 14:207–15. <https://doi.org/10.1016/j.chom.2013.07.007> PMID: 23954159
9. Han YW, Shi W, Huang GT, Kinder Haake S, Park NH, Kuramitsu H, et al. Interactions between periodontal bacteria and human oral epithelial cells: *Fusobacterium nucleatum* adheres to and invades epithelial cells. *Infect Immun* 2000; 68:3140–6. <https://doi.org/10.1128/IAI.68.6.3140-3146.2000> PMID: 10816455
10. Liu B, Faller LL, Klitgord N, Mazumdar V, Ghodsi M, Sommer DD, et al. Deep Sequencing of the Oral Microbiome Reveals Signatures of Periodontal Disease. *PLoS ONE* 2012; 7:e37919. <https://doi.org/10.1371/journal.pone.0037919> PMID: 22675498

11. Zhang N, Liu Y, Yang H, Liang M, Wang X, Wang M, et al. Clinical Significance of *Fusobacterium nucleatum* Infection and Regulatory T Cell Enrichment in Esophageal Squamous Cell Carcinoma. *Pathol Oncol Res* 2021; 27:1609846. <https://doi.org/10.3389/pore.2021.1609846> PMID: 34305476
12. Nomoto D, Baba Y, Liu Y, Tsutsuki H, Okadome K, Harada K, et al. *Fusobacterium nucleatum* promotes esophageal squamous cell carcinoma progression via the NOD1/RIPK2/NF- κ B pathway. *Cancer Lett* 2022; 530:59–67. <https://doi.org/10.1016/j.canlet.2022.01.014>.
13. Parhi L, Alon-Maimon T, Sol A, Nejman D, Shhadeh A, Fainsod-Levi T, et al. Breast cancer colonization by *Fusobacterium nucleatum* accelerates tumor growth and metastatic progression. *Nat Commun* 2020; 11:3259. <https://doi.org/10.1038/s41467-020-16967-2> PMID: 32591509
14. Dejea CM, Wick EC, Hechenbleikner EM, White JR, Mark Welch JL, Rossetti BJ, et al. Microbiota organization is a distinct feature of proximal colorectal cancers. *Proc Natl Acad Sci U S A* 2014; 111:18321–6. <https://doi.org/10.1073/pnas.1406199111> PMID: 25489084
15. Dejea CM, Fathi P, Craig JM, Boleij A, Taddese R, Geis AL, et al. Patients with familial adenomatous polyposis harbor colonic biofilms containing tumorigenic bacteria. *Science* 2018; 359:592–7. <https://doi.org/10.1126/science.aah3648> PMID: 29420293
16. Yu TC, Guo F, Yu Y, Sun T, Ma D, Han J, et al. *Fusobacterium nucleatum* Promotes Chemoresistance to Colorectal Cancer by Modulating Autophagy. *Cell* 2017; 170:548–563.e16. <https://doi.org/10.1016/j.cell.2017.07.008> PMID: 28753429
17. Wang S, Liu Y, Li J, Zhao L, Yan W, Lin B, et al. *Fusobacterium nucleatum* Acts as a Pro-carcinogenic Bacterium in Colorectal Cancer: From Association to Causality. *Front Cell Dev Biol* 2021; 9:710165. <https://doi.org/10.3389/fcell.2021.710165> PMID: 34490259
18. Gao Y, Bi D, Xie R, Li M, Guo J, Liu H, et al. *Fusobacterium nucleatum* enhances the efficacy of PD-L1 blockade in colorectal cancer. *Sig Transduct Target Ther* 2021; 6:1–10. <https://doi.org/10.1038/s41392-021-00795-x>.
19. Ikegami A, Chung P, Han YW. Complementation of the *fadA* mutation in *Fusobacterium nucleatum* demonstrates that the surface-exposed adhesin promotes cellular invasion and placental colonization. *Infect Immun* 2009; 77:3075–9. <https://doi.org/10.1128/IAI.00209-09> PMID: 19398541
20. Meng Q, Gao Q, Mehrazarin S, Tangwanichgapong K, Wang Y, Huang Y, et al. *Fusobacterium nucleatum* secretes amyloid-like *FadA* to enhance pathogenicity. *EMBO Rep* 2021; 22:e52891. <https://doi.org/10.15252/embr.202152891> PMID: 34184813
21. Copenhagen-Glazer S, Sol A, Abed J, Naor R, Zhang X, Han YW, et al. *Fap2* of *Fusobacterium nucleatum* is a galactose-inhibitable adhesin involved in coaggregation, cell adhesion, and preterm birth. *Infect Immun* 2015; 83:1104–13. <https://doi.org/10.1128/IAI.02838-14> PMID: 25561710
22. Abed J, Emgård JEM, Zamir G, Faroja M, Almogy G, Grenov A, et al. *Fap2* Mediates *Fusobacterium nucleatum* Colorectal Adenocarcinoma Enrichment by Binding to Tumor-Expressed Gal-GalNAc. *Cell Host Microbe* 2016; 20:215–25. <https://doi.org/10.1016/j.chom.2016.07.006> PMID: 27512904
23. Yang GY, Shamsuddin AM. Gal-GalNAc: a biomarker of colon carcinogenesis. *Histol Histopathol* 1996; 11:801–6. PMID: 8839767
24. Gur C, Ibrahim Y, Isaacson B, Yamin R, Abed J, Gamliel M, et al. Binding of the *Fap2* protein of *Fusobacterium nucleatum* to human inhibitory receptor TIGIT protects tumors from immune cell attack. *Immunity* 2015; 42:344–55. <https://doi.org/10.1016/j.immuni.2015.01.010> PMID: 25680274
25. Guo P, Tian Z, Kong X, Yang L, Shan X, Dong B, et al. *FadA* promotes DNA damage and progression of *Fusobacterium nucleatum*-induced colorectal cancer through up-regulation of *chk2*. *J Exp Clin Cancer Res* 2020; 39:202. <https://doi.org/10.1186/s13046-020-01677-w> PMID: 32993749
26. Rubinstein MR, Wang X, Liu W, Hao Y, Cai G, Han YW. *Fusobacterium nucleatum* promotes colorectal carcinogenesis by modulating E-cadherin/ β -catenin signaling via its *FadA* adhesin. *Cell Host Microbe* 2013; 14:195–206. <https://doi.org/10.1016/j.chom.2013.07.012>.
27. Rubinstein MR, Baik JE, Lagana SM, Han RP, Raab WJ, Sahoo D, et al. *Fusobacterium nucleatum* promotes colorectal cancer by inducing Wnt/ β -catenin modulator Annexin A1. *EMBO Rep* 2019; 20:e47638. <https://doi.org/10.15252/embr.201847638>.
28. Wang N, Fang J-Y. *Fusobacterium nucleatum*, a key pathogenic factor and microbial biomarker for colorectal cancer. *Trends in Microbiology* 2022; 0. <https://doi.org/10.1016/j.tim.2022.08.010> PMID: 36058786
29. Prindiville TP, Sheikh RA, Cohen SH, Tang YJ, Cantrell MC, Silva J. *Bacteroides fragilis* enterotoxin gene sequences in patients with inflammatory bowel disease. *Emerg Infect Dis* 2000; 6:171–4. <https://doi.org/10.3201/eid0602.000210> PMID: 10756151
30. Rabizadeh S, Rhee K-J, Wu S, Huso D, Gan CM, Golub JE, et al. Enterotoxigenic *Bacteroides fragilis*: A Potential Instigator of Colitis. *Inflamm Bowel Dis* 2007; 13:1475–83. <https://doi.org/10.1002/ibd.20265> PMID: 17886290

31. Cao Y, Wang Z, Yan Y, Ji L, He J, Xuan B, et al. Enterotoxigenic *Bacteroides fragilis* Promotes Intestinal Inflammation and Malignancy by Inhibiting Exosome-Packaged miR-149-3p. *Gastroenterology* 2021; 161:1552–1566.e12. <https://doi.org/10.1053/j.gastro.2021.08.003> PMID: 34371001
32. Sears CL, Islam S, Saha A, Arjumand M, Alam NH, Faruque ASG, et al. Association of Enterotoxigenic *Bacteroides fragilis* Infection with Inflammatory Diarrhea. *Clin Infect Dis* 2008; 47:797–803. <https://doi.org/10.1086/591130> PMID: 18680416
33. Shang S, Hua F, Hu Z-W. The regulation of β -catenin activity and function in cancer: therapeutic opportunities. *Oncotarget* 2017; 8:33972–89. <https://doi.org/10.18632/oncotarget.15687>.
34. Wu S, Morin PJ, Maouyo D, Sears CL. *Bacteroides fragilis* enterotoxin induces c-Myc expression and cellular proliferation. *Gastroenterology* 2003; 124:392–400. <https://doi.org/10.1053/gast.2003.50047> PMID: 12557145
35. Wu S, Shin J, Zhang G, Cohen M, Franco A, Sears CL. The *Bacteroides fragilis* toxin binds to a specific intestinal epithelial cell receptor. *Infection and Immunity* 2006; 74:5382–90. <https://doi.org/10.1128/IAI.00060-06> PMID: 16926433
36. Toprak NU, Yagci A, Gulluoglu BM, Akin ML, Demirkalem P, Celenk T, et al. A possible role of *Bacteroides fragilis* enterotoxin in the aetiology of colorectal cancer. *Clin Microbiol Infect* 2006; 12:782–6. <https://doi.org/10.1111/j.1469-0691.2006.01494.x> PMID: 16842574
37. Geis A, Dejea C, Fan H, Wu X, Wu S, Huso D, et al. Enterotoxigenic *Bacteroides fragilis* induces oncogenic regulatory T cells (TUM9P.1000). *The Journal of Immunology* 2015; 194:210.2–210.2.
38. Geis AL, Fan H, Wu X, Wu S, Huso DL, Wolfe JL, et al. Regulatory T cell response to enterotoxigenic *Bacteroides fragilis* colonization triggers IL-17-dependent colon carcinogenesis. *Cancer Discov* 2015; 5:1098–109. <https://doi.org/10.1158/2159-8290.CD-15-0447> PMID: 26201900
39. Housseau F, Wu S, Wick EC, Fan H, Wu X, Llosa NJ, et al. Redundant innate and adaptive sources of IL-17 production drive colon tumorigenesis. *Cancer Res* 2016; 76:2115–24. <https://doi.org/10.1158/0008-5472.CAN-15-0749> PMID: 26880802
40. Thiele Orberg E, Fan H, Tam AJ, Dejea CM, Destefano Shields CE, Wu S, et al. The myeloid immune signature of enterotoxigenic *Bacteroides fragilis*-induced murine colon tumorigenesis. *Mucosal Immunology* 2017; 10:421–33. <https://doi.org/10.1038/mi.2016.53> PMID: 27301879
41. Moser AR, Luongo C, Gould KA, McNeley MK, Shoemaker AR, Dove WF. ApcMin: a mouse model for intestinal and mammary tumorigenesis. *Eur J Cancer* 1995; 31A:1061–4. [https://doi.org/10.1016/0959-8049\(95\)00181-h](https://doi.org/10.1016/0959-8049(95)00181-h) PMID: 7576992
42. Kwong LN, Dove WF. APC and its modifiers in colon cancer. *Adv Exp Med Biol* 2009; 656:85–106. https://doi.org/10.1007/978-1-4419-1145-2_8 PMID: 19928355
43. Nguyen HT, Duong H-Q. The molecular characteristics of colorectal cancer: Implications for diagnosis and therapy (Review). *Oncology Letters* 2018; 16:9–18. <https://doi.org/10.3892/ol.2018.8679>.
44. Housseau F, Sears CL. Enterotoxigenic *Bacteroides fragilis* (ETBF)-mediated colitis in Min (Apc^{+/-}) mice: A human commensal-based murine model of colon carcinogenesis. *Cell Cycle* 2010; 9:3–5. <https://doi.org/10.4161/cc.9.1.10352> PMID: 20009569
45. Chung L, Thiele Orberg E, Geis AL, Chan JL, Fu K, DeStefano Shields CE, et al. *Bacteroides fragilis* Toxin Coordinates a Pro-carcinogenic Inflammatory Cascade via Targeting of Colonic Epithelial Cells. *Cell Host and Microbe* 2018; 23:203–214.e5. <https://doi.org/10.1016/j.chom.2018.01.007> PMID: 29398651
46. Yang Y, Weng W, Peng J, Hong L, Yang L, Toiyama Y, et al. *Fusobacterium nucleatum* Increases Proliferation of Colorectal Cancer Cells and Tumor Development in Mice by Activating Toll-Like Receptor 4 Signaling to Nuclear Factor- κ B, and Up-regulating Expression of MicroRNA-21. *Gastroenterology* 2017; 152:851–866.e24. <https://doi.org/10.1053/j.gastro.2016.11.018>.
47. Allen J, Rosendahl Huber A, Pleguezuelos-Manzano C, Puschhof J, Wu S, Wu X, et al. Colon Tumors in Enterotoxigenic *Bacteroides fragilis* (ETBF)-Colonized Mice Do Not Display a Unique Mutational Signature but Instead Possess Host-Dependent Alterations in the APC Gene. *Microbiology Spectrum* 2022; 10:e01055–22. <https://doi.org/10.1128/spectrum.01055-22> PMID: 35587635
48. Lu SSM, Mohammed Z, Häggström C, Myte R, Lindquist E, Gylfe Å, et al. Antibiotics Use and Subsequent Risk of Colorectal Cancer: A Swedish Nationwide Population-Based Study. *JNCI: Journal of the National Cancer Institute* 2022; 114:38–46. <https://doi.org/10.1093/jnci/djab125>.
49. Zhang J, Haines C, Watson AJM, Hart AR, Platt MJ, Pardoll DM, et al. Oral antibiotic use and risk of colorectal cancer in the United Kingdom, 1989–2012: a matched case-control study. *Gut* 2019; 68:1971–8. <https://doi.org/10.1136/gutjnl-2019-318593> PMID: 31427405
50. Armstrong D, Dregan A, Ashworth M, White P, McGee C, de Lusignan S. The association between colorectal cancer and prior antibiotic prescriptions: case control study. *Br J Cancer* 2020; 122:912–7. <https://doi.org/10.1038/s41416-019-0701-5> PMID: 31929515

51. Yang Y, Weng W, Peng J, Hong L, Yang L, Toiyama Y, et al. *Fusobacterium nucleatum* Increases Proliferation of Colorectal Cancer Cells and Tumor Development in Mice by Activating TLR4 Signaling to NF κ B, Upregulating Expression of microRNA-21. *Gastroenterology* 2017; 152:851–866.e24. <https://doi.org/10.1053/j.gastro.2016.11.018>.
52. Orberg ET, Fan H, Tam AJ, Dejea CM, Destefano-Shields CE, Wu S, et al. The Myeloid Immune Signature of Enterotoxigenic *Bacteroides Fragilis*-Induced Murine Colon Tumorigenesis. *Mucosal Immunol* 2017; 10:421–33. <https://doi.org/10.1038/mi.2016.53> PMID: 27301879
53. Wong SH, Kwong TNY, Chow T-C, Luk AKC, Dai RZW, Nakatsu G, et al. Quantitation of faecal *Fusobacterium* improves faecal immunochemical test in detecting advanced colorectal neoplasia. *Gut* 2017; 66:1441–8. <https://doi.org/10.1136/gutjnl-2016-312766> PMID: 27797940
54. Zhang M, Lv Y, Hou S, Liu Y, Wang Y, Wan X. Differential Mucosal Microbiome Profiles across Stages of Human Colorectal Cancer. *Life (Basel)* 2021; 11:831. <https://doi.org/10.3390/life11080831> PMID: 34440574
55. Purcell RV, Visnovska M, Biggs PJ, Schmeier S, Frizelle FA. Distinct gut microbiome patterns associate with consensus molecular subtypes of colorectal cancer. *Scientific Reports* 2017; 7:1–12. <https://doi.org/10.1038/s41598-017-11237-6>.
56. Zamani S, Taslimi R, Sarabi A, Jasemi S, Sechi LA, Feizabadi MM. Enterotoxigenic *Bacteroides fragilis*: A Possible Etiological Candidate for Bacterially-Induced Colorectal Precancerous and Cancerous Lesions. *Frontiers in Cellular and Infection Microbiology* 2020; 9. <https://doi.org/10.3389/fcimb.2019.00449> PMID: 32010637
57. Tjalsma H, Boleij A, Marchesi JR, Dutilh BE. A bacterial driver-passenger model for colorectal cancer: beyond the usual suspects. *Nat Rev Microbiol* 2012; 10:575–82. <https://doi.org/10.1038/nrmicro2819> PMID: 22728587
58. Hao Y, Hao S, Andersen-Nissen E, Mauck WM, Zheng S, Butler A, et al. Integrated analysis of multi-modal single-cell data. *Cell* 2021; 184:3573–3587.e29. <https://doi.org/10.1016/j.cell.2021.04.048> PMID: 34062119
59. Haber AL, Biton M, Rogel N, Herbst RH, Shekhar K, Smillie C, et al. A single-cell survey of the small intestinal epithelium. *Nature* 2017; 551:333–9. <https://doi.org/10.1038/nature24489> PMID: 29144463
60. Moor AE, Harnik Y, Ben-Moshe S, Massasa EE, Rozenberg M, Eilam R, et al. Spatial Reconstruction of Single Enterocytes Uncovers Broad Zonation along the Intestinal Villus Axis. *Cell* 2018; 175:1156–1167.e15. <https://doi.org/10.1016/j.cell.2018.08.063> PMID: 30270040
61. Li J, Sheng Q, Shyr Y, Liu Q. scMRMA: single cell multiresolution marker-based annotation. *Nucleic Acids Research* 2022; 50:e7. <https://doi.org/10.1093/nar/gkab931> PMID: 34648021
62. Huels DJ, Sansom OJ. Stem vs non-stem cell origin of colorectal cancer. *Br J Cancer* 2015; 113:1–5. <https://doi.org/10.1038/bjc.2015.214> PMID: 26110974
63. Liu H, Du J, Chao S, Li S, Cai H, Zhang H, et al. *Fusobacterium nucleatum* Promotes Colorectal Cancer Cell to Acquire Stem Cell-Like Features by Manipulating Lipid Droplet-Mediated Numb Degradation. *Adv Sci (Weinh)* 2022; 9:2105222. <https://doi.org/10.1002/advs.202105222> PMID: 35170250
64. Wang Q, Yu C, Yue C, Liu X. *Fusobacterium nucleatum* produces cancer stem cell characteristics via EMT-resembling variations. *Int J Clin Exp Pathol* 2020; 13:1819–28. PMID: 32782710
65. Liu Q-Q, Li C-M, Fu L-N, Wang H-L, Tan J, Wang Y-Q, et al. Enterotoxigenic *Bacteroides fragilis* induces the stemness in colorectal cancer via upregulating histone demethylase JMJD2B. *Gut Microbes* n.d.; 12:1788900. <https://doi.org/10.1080/19490976.2020.1788900> PMID: 32684087
66. Zhou Y, Xia L, Wang H, Oyang L, Su M, Liu Q, et al. Cancer stem cells in progression of colorectal cancer. *Oncotarget* 2017; 9:33403–15. <https://doi.org/10.18632/oncotarget.23607> PMID: 30279970
67. Munro MJ, Wickremesekera SK, Peng L, Tan ST, Itinteang T. Cancer stem cells in colorectal cancer: a review. *Journal of Clinical Pathology* 2018; 71:110–6. <https://doi.org/10.1136/jclinpath-2017-204739> PMID: 28942428
68. Becker WR, Nevins SA, Chen DC, Chiu R, Horning AM, Guha TK, et al. Single-cell analyses define a continuum of cell state and composition changes in the malignant transformation of polyps to colorectal cancer. *Nat Genet* 2022; 54:985–95. <https://doi.org/10.1038/s41588-022-01088-x> PMID: 35726067
69. Wang H, Gong P, Chen T, Gao S, Wu Z, Wang X, et al. Colorectal Cancer Stem Cell States Uncovered by Simultaneous Single-Cell Analysis of Transcriptome and Telomeres. *Adv Sci (Weinh)* 2021; 8:2004320. <https://doi.org/10.1002/advs.202004320> PMID: 33898197
70. Yue M, Yun Z, Li S, Yan G, Kang Z. NEDD4 triggers FOXA1 ubiquitination and promotes colon cancer progression under microRNA-340-5p suppression and ATF1 upregulation. *RNA Biology* 2021; 18:1981–95. <https://doi.org/10.1080/15476286.2021.1885232> PMID: 33530829

71. Lazar SB, Pongor L, Li XL, Grammatikakis I, Muys BR, Dangelmaier EA, et al. Genome-Wide Analysis of the FOXA1 Transcriptional Network Identifies Novel Protein-Coding and Long Noncoding RNA Targets in Colorectal Cancer Cells. *Mol Cell Biol* 2020; 40:e00224–20. <https://doi.org/10.1128/MCB.00224-20> PMID: 32839292
72. Park Y-L, Kim S-H, Park S-Y, Jung M-W, Ha S-Y, Choi J-H, et al. Forkhead-box A1 regulates tumor cell growth and predicts prognosis in colorectal cancer. *Int J Oncol* 2019; 54:2169–78. <https://doi.org/10.3892/ijo.2019.4771>.
73. Wang B, Li Y, Tan F, Xiao Z. Increased expression of SOX4 is associated with colorectal cancer progression. *Tumour Biol* 2016; 37:9131–7. <https://doi.org/10.1007/s13277-015-4756-5> PMID: 26768610
74. Liu J, Qiu J, Zhang Z, Zhou L, Li Y, Ding D, et al. SOX4 maintains the stemness of cancer cells via transcriptionally enhancing HDAC1 revealed by comparative proteomics study. *Cell & Bioscience* 2021; 11:23. <https://doi.org/10.1186/s13578-021-00539-y> PMID: 33482915
75. Petrova TV, Nykänen A, Norrmén C, Ivanov KI, Andersson LC, Haglund C, et al. Transcription factor PROX1 induces colon cancer progression by promoting the transition from benign to highly dysplastic phenotype. *Cancer Cell* 2008; 13:407–19. <https://doi.org/10.1016/j.ccr.2008.02.020> PMID: 18455124
76. Ragusa S, Cheng J, Ivanov KI, Zangger N, Ceteci F, Bernier-Latmani J, et al. PROX1 promotes metabolic adaptation and fuels outgrowth of Wnt(high) metastatic colon cancer cells. *Cell Rep* 2014; 8:1957–73. <https://doi.org/10.1016/j.celrep.2014.08.041> PMID: 25242332
77. Wiener Z, Högström J, Hyvönen V, Band AM, Kallio P, Holopainen T, et al. Prox1 promotes expansion of the colorectal cancer stem cell population to fuel tumor growth and ischemia resistance. *Cell Reports* 2014; 8:1943–56. <https://doi.org/10.1016/j.celrep.2014.08.034> PMID: 25242330
78. Fevr T, Robine S, Louvard D, Huelsken J. Wnt/ β -Catenin Is Essential for Intestinal Homeostasis and Maintenance of Intestinal Stem Cells. *Molecular and Cellular Biology* 2007; 27:7551–9. <https://doi.org/10.1128/MCB.01034-07>.
79. Li B, Lee C, Cadete M, Zhu H, Koike Y, Hock A, et al. Impaired Wnt/ β -catenin pathway leads to dysfunction of intestinal regeneration during necrotizing enterocolitis. *Cell Death Dis* 2019; 10:1–11. <https://doi.org/10.1038/s41419-019-1987-1>.
80. Gregorieff A, Clevers H. Wnt signaling in the intestinal epithelium: from endoderm to cancer. *Genes Dev* 2005; 19:877–90. <https://doi.org/10.1101/gad.1295405> PMID: 15833914
81. Zheng C-C, Hu H-F, Hong P, Zhang Q-H, Xu WW, He Q-Y, et al. Significance of integrin-linked kinase (ILK) in tumorigenesis and its potential implication as a biomarker and therapeutic target for human cancer. *Am J Cancer Res* 2019; 9:186–97. PMID: 30755822
82. Tsoumas D, Nikou S, Giannopoulou E, Champeris Tsaniras S, Sirinian C, Maroulis I, et al. ILK Expression in Colorectal Cancer Is Associated with EMT, Cancer Stem Cell Markers and Chemoresistance. *Cancer Genomics Proteomics* 2018; 15:127–41. <https://doi.org/10.21873/cgp.20071> PMID: 29496692
83. Almasabi S, Ahmed AU, Boyd R, Williams BRG. A Potential Role for Integrin-Linked Kinase in Colorectal Cancer Growth and Progression via Regulating Senescence and Immunity. *Front Genet* 2021; 12:638558. <https://doi.org/10.3389/fgene.2021.638558> PMID: 34163519
84. Huang L, Fang X, Shi D, Yao S, Wu W, Fang Q, et al. MSP-RON Pathway: Potential Regulator of Inflammation and Innate Immunity. *Front Immunol* 2020; 11:569082. <https://doi.org/10.3389/fimmu.2020.569082> PMID: 33117355
85. Li C, Morvaridi S, Lam G, Chheda C, Kamata Y, Katsumata M, et al. MSP-RON Signaling Is Activated in the Transition From Pancreatic Intraepithelial Neoplasia (PanIN) to Pancreatic Ductal Adenocarcinoma (PDAC). *Frontiers in Physiology* 2019; 10. <https://doi.org/10.3389/fphys.2019.00147> PMID: 30863319
86. Yao H-P, Zhou Y-Q, Zhang R, Wang M-H. MSP-RON signalling in cancer: pathogenesis and therapeutic potential. *Nature Reviews Cancer* 2013; 13:466–82. <https://doi.org/10.1038/nrc3545> PMID: 23792360
87. Li J, Ma X, Chakravarti D, Shalpour S, DePinho RA. Genetic and biological hallmarks of colorectal cancer. *Genes Dev* 2021; 35:787–820. <https://doi.org/10.1101/gad.348226.120> PMID: 34074695
88. Bao Y, Tang J, Qian Y, Sun T, Chen H, Chen Z, et al. Long noncoding RNA BFAL1 mediates enterotoxigenic *Bacteroides fragilis*-related carcinogenesis in colorectal cancer via the RHEB/mTOR pathway. *Cell Death and Disease* 2019; 10. <https://doi.org/10.1038/s41419-019-1925-2> PMID: 31515468
89. Purcell RV, Permain J, Keenan JI. Enterotoxigenic *Bacteroides fragilis* activates IL-8 expression through Stat3 in colorectal cancer cells. *Gut Pathog* 2022; 14:16. <https://doi.org/10.1186/s13099-022-00489-x> PMID: 35468857
90. Ghaleb AM, Yang VW. The Pathobiology of Krüppel-like Factors in Colorectal Cancer. *Curr Colorectal Cancer Rep* 2008; 4:59–64.

91. Cao D, Hou M, Guan Y, Jiang M, Yang Y, Gou H. Expression of HIF-1alpha and VEGF in colorectal cancer: association with clinical outcomes and prognostic implications. *BMC Cancer* 2009; 9:432. <https://doi.org/10.1186/1471-2407-9-432> PMID: 20003271
92. Corvinus FM, Orth C, Moriggl R, Tsareva SA, Wagner S, Pfitzner EB, et al. Persistent STAT3 Activation in Colon Cancer Is Associated with Enhanced Cell Proliferation and Tumor Growth. *Neoplasia* 2005; 7:545–55. <https://doi.org/10.1593/neo.04571> PMID: 16036105
93. Borst J, Ahrends T, Bąbala N, Melief CJM, Kastenmüller W. CD4+ T cell help in cancer immunology and immunotherapy. *Nat Rev Immunol* 2018; 18:635–47. <https://doi.org/10.1038/s41577-018-0044-0> PMID: 30057419
94. Philip M, Schietinger A. CD8+ T cell differentiation and dysfunction in cancer. *Nat Rev Immunol* 2022; 22:209–23. <https://doi.org/10.1038/s41577-021-00574-3> PMID: 34253904
95. Di J, Liu M, Fan Y, Gao P, Wang Z, Jiang B, et al. Phenotype molding of T cells in colorectal cancer by single-cell analysis. *International Journal of Cancer* 2020; 146:2281–95. <https://doi.org/10.1002/ijc.32856> PMID: 31901134
96. Zhang L, Yu X, Zheng L, Zhang Y, Li Y, Fang Q, et al. Lineage tracking reveals dynamic relationships of T cells in colorectal cancer. *Nature* 2018; 564:268–72. <https://doi.org/10.1038/s41586-018-0694-x> PMID: 30479382
97. Kim CG, Jang M, Kim Y, Leem G, Kim KH, Lee H, et al. VEGF-A drives TOX-dependent T cell exhaustion in anti-PD-1-resistant microsatellite stable colorectal cancers. *Science Immunology* 2019; 4: eaay0555. <https://doi.org/10.1126/sciimmunol.aay0555> PMID: 31704735
98. Geis AL, Housseau F. Procarcinogenic regulatory T cells in microbial-induced colon cancer. *Onc Immunology* 2016; 5:e1118601. <https://doi.org/10.1080/2162402X.2015.1118601> PMID: 27141400
99. Mima K, Sukawa Y, Nishihara R, Qian ZR, Yamauchi M, Inamura K, et al. *Fusobacterium nucleatum* and T Cells in Colorectal Carcinoma. *JAMA Oncol* 2015; 1:653–61. <https://doi.org/10.1001/jamaoncol.2015.1377> PMID: 26181352
100. Galaski J, Shhadeh A, Umaña A, Yoo CC, Arpinati L, Isaacson B, et al. *Fusobacterium nucleatum* CbpF Mediates Inhibition of T Cell Function Through CEACAM1 Activation. *Frontiers in Cellular and Infection Microbiology* 2021; 11. <https://doi.org/10.3389/fcimb.2021.692544> PMID: 34336716
101. Cullen SP, Brunet M, Martin SJ. Granzymes in cancer and immunity. *Cell Death Differ* 2010; 17:616–23. <https://doi.org/10.1038/cdd.2009.206> PMID: 20075940
102. Trapani JA. Granzymes: a family of lymphocyte granule serine proteases. *Genome Biol* 2001; 2: reviews3014.1–reviews3014.7. <https://doi.org/10.1186/gb-2001-2-12-reviews3014> PMID: 11790262
103. Wang B, Wang Y, Sun X, Deng G, Huang W, Wu X, et al. CXCR6 is required for antitumor efficacy of intratumoral CD8+ T cell. *J Immunother Cancer* 2021; 9:e003100. <https://doi.org/10.1136/jitc-2021-003100> PMID: 34462326
104. Muthuswamy R, McGray AR, Battaglia S, He W, Miliotto A, Eppolito C, et al. CXCR6 by increasing retention of memory CD8+ T cells in the ovarian tumor microenvironment promotes immunosurveillance and control of ovarian cancer. *J Immunother Cancer* 2021; 9:e003329. <https://doi.org/10.1136/jitc-2021-003329> PMID: 34607898
105. Di Pilato M, Kfuri-Rubens R, Pruessmann JN, Ozga AJ, Messemaker M, Cadilha BL, et al. CXCR6 positions cytotoxic T cells to receive critical survival signals in the tumor microenvironment. *Cell* 2021; 184:4512–4530.e22. <https://doi.org/10.1016/j.cell.2021.07.015>.
106. Pan P-Y, Zang Y, Weber K, Meseck ML, Chen S-H. OX40 ligation enhances primary and memory cytotoxic T lymphocyte responses in an immunotherapy for hepatic colon metastases. *Mol Ther* 2002; 6:528–36. <https://doi.org/10.1006/mthe.2002.0699> PMID: 12377195
107. Pham Minh N, Murata S, Kitamura N, Ueki T, Kojima M, Miyake T, et al. In vivo antitumor function of tumor antigen-specific CTLs generated in the presence of OX40 co-stimulation in vitro. *Int J Cancer* 2018; 142:2335–43. <https://doi.org/10.1002/ijc.31244> PMID: 29313971
108. Bansal-Pakala P, Halteman BS, Cheng MH-Y, Croft M. Costimulation of CD8 T Cell Responses by OX40. *The Journal of Immunology* 2004; 172:4821–5. <https://doi.org/10.4049/jimmunol.172.8.4821> PMID: 15067059
109. Wirbel J, Pyl PT, Kartal E, Zych K, Kashani A, Milanese A, et al. Meta-analysis of fecal metagenomes reveals global microbial signatures that are specific for colorectal cancer. *Nat Med* 2019; 25:679–89. <https://doi.org/10.1038/s41591-019-0406-6> PMID: 30936547
110. Thomas AM, Manghi P, Asnicar F, Pasolli E, Armanini F, Zolfo M, et al. Metagenomic analysis of colorectal cancer datasets identifies cross-cohort microbial diagnostic signatures and a link with choline degradation. *Nat Med* 2019; 25:667–78. <https://doi.org/10.1038/s41591-019-0405-7> PMID: 30936548

111. Yachida S, Mizutani S, Shiroma H, Shiba S, Nakajima T, Sakamoto T, et al. Metagenomic and metabolomic analyses reveal distinct stage-specific phenotypes of the gut microbiota in colorectal cancer. *Nature Medicine* 2019; 25:968–76. <https://doi.org/10.1038/s41591-019-0458-7> PMID: 31171880
112. Sepich-poore GD, Zitvogel L, Straussman R, Hasty J, Wargo JA, Knight R. The microbiome and human cancer 2021; 4552. <https://doi.org/10.1126/science.abc4552>.
113. Muzny DM, Bainbridge MN, Chang K, Dinh HH, Drummond JA, Fowler G, et al. Comprehensive molecular characterization of human colon and rectal cancer. *Nature* 2012; 487:330–7. <https://doi.org/10.1038/nature11252> PMID: 22810696
114. Byun A, Hung KE, Fleet JC, Bronson RT, Mason JB, Garcia PE, et al. Colon-specific tumorigenesis in mice driven by Cre-mediated inactivation of Apc and activation of mutant Kras. *Cancer Lett* 2014; 347:191–5. <https://doi.org/10.1016/j.canlet.2014.03.004> PMID: 24632531
115. Knippel RJ, Drewes JL, Sears CL. The Cancer Microbiome: Recent Highlights and Knowledge Gaps. *Cancer Discov* 2021; 11:2378–95. <https://doi.org/10.1158/2159-8290.CD-21-0324> PMID: 34400408
116. Sears CL, Garrett WS. Microbes, Microbiota, and Colon Cancer. *Cell Host & Microbe* 2014; 15:317–28. <https://doi.org/10.1016/j.chom.2014.02.007> PMID: 24629338
117. Hatakeyama M. Helicobacter pylori CagA and Gastric Cancer: A Paradigm for Hit-and-Run Carcinogenesis. *Cell Host & Microbe* 2014; 15:306–16. <https://doi.org/10.1016/j.chom.2014.02.008> PMID: 24629337
118. Ternes D, Karta J, Tsenkova M, Wilmes P, Haan S, Letellier E. Microbiome in Colorectal Cancer: How to Get from Meta-omics to Mechanism? *Trends in Microbiology* 2020; 28:401–23. <https://doi.org/10.1016/j.tim.2020.01.001> PMID: 32298617
119. van den Brink SC, Sage F, Vértesy Á, Spanjaard B, Peterson-Maduro J, Baron CS, et al. Single-cell sequencing reveals dissociation-induced gene expression in tissue subpopulations. *Nat Methods* 2017; 14:935–6. <https://doi.org/10.1038/nmeth.4437> PMID: 28960196
120. Khan I, Bai Y, Zha L, Ullah N, Ullah H, Shah SRH, et al. Mechanism of the Gut Microbiota Colonization Resistance and Enteric Pathogen Infection. *Frontiers in Cellular and Infection Microbiology* 2021; 11. <https://doi.org/10.3389/fcimb.2021.716299> PMID: 35004340
121. Lawley TD, Walker AW. Intestinal colonization resistance. *Immunology* 2013; 138:1–11. <https://doi.org/10.1111/j.1365-2567.2012.03616.x> PMID: 23240815
122. Ley RE, Peterson DA, Gordon JL. Ecological and Evolutionary Forces Shaping Microbial Diversity in the Human Intestine. *Cell* 2006; 124:837–48. <https://doi.org/10.1016/j.cell.2006.02.017> PMID: 16497592
123. Ma H, Tao W, Zhu S. T lymphocytes in the intestinal mucosa: defense and tolerance. *Cell Mol Immunol* 2019; 16:216–24. <https://doi.org/10.1038/s41423-019-0208-2> PMID: 30787416
124. Yip JLK, Balasuriya GK, Spencer SJ, Hill-Yardin EL. The Role of Intestinal Macrophages in Gastrointestinal Homeostasis: Heterogeneity and Implications in Disease. *Cell Mol Gastroenterol Hepatol* 2021; 12:1701–18. <https://doi.org/10.1016/j.jcmgh.2021.08.021> PMID: 34506953
125. Pleguezuelos-Manzano C, Puschhof J, Rosendahl Huber A, van Hoesck A, Wood HM, Nomburg J, et al. Mutational signature in colorectal cancer caused by genotoxic pks + E. coli. *Nature* 2020; 580:269–73. <https://doi.org/10.1038/s41586-020-2080-8> PMID: 32106218
126. Cuevas-Ramos G, Petit CR, Marcq I, Boury M, Oswald E, Nougayrède JP. Escherichia coli induces DNA damage in vivo and triggers genomic instability in mammalian cells. *Proceedings of the National Academy of Sciences of the United States of America* 2010; 107:11537–42. <https://doi.org/10.1073/pnas.1001261107> PMID: 20534522
127. Iftexhar A, Berger H, Bouznad N, Heuberger J, Boccellato F, Dobrindt U, et al. Genomic aberrations after short-term exposure to colibactin-producing E. coli transform primary colon epithelial cells. *Nat Commun* 2021; 12:1003. <https://doi.org/10.1038/s41467-021-21162-y> PMID: 33579932
128. Tomkovich S, Dejea CM, Winglee K, Drewes JL, Chung L, Housseau F, et al. Human colon mucosal biofilms from healthy or colon cancer hosts are carcinogenic. *J Clin Invest* n.d.; 129:1699–712. <https://doi.org/10.1172/JCI124196>.
129. Yang Y, Misra BB, Liang L, Bi D, Weng W, Wu W, et al. Integrated microbiome and metabolome analysis reveals a novel interplay between commensal bacteria and metabolites in colorectal cancer. *Theranostics* 2019; 9:4101–14. <https://doi.org/10.7150/thno.35186> PMID: 31281534
130. Dai Z, Coker OO, Nakatsu G, Wu WKK, Zhao L, Chen Z, et al. Multi-cohort analysis of colorectal cancer metagenome identified altered bacteria across populations and universal bacterial markers. *Microbiome* 2018; 6:70–70. <https://doi.org/10.1186/s40168-018-0451-2> PMID: 29642940
131. Zhao L, Zhang X, Zhou Y, Fu K, Lau HC-H, Chun TW-Y, et al. Parvimonas micra promotes colorectal tumorigenesis and is associated with prognosis of colorectal cancer patients. *Oncogene* 2022; 41:4200–10. <https://doi.org/10.1038/s41388-022-02395-7> PMID: 35882981

132. Tsoi H, Chu ESH, Zhang X, Sheng J, Nakatsu G, Ng SC, et al. *Peptostreptococcus anaerobius* Induces Intracellular Cholesterol Biosynthesis in Colon Cells to Induce Proliferation and Causes Dysplasia in Mice. *Gastroenterology* 2017; 152:1419–1433.e5. <https://doi.org/10.1053/j.gastro.2017.01.009> PMID: 28126350
133. Drewes JL, White JR, Dejea CM, Fathi P, Iyadorai T, Vadivelu J, et al. High-resolution bacterial 16S rRNA gene profile meta-analysis and biofilm status reveal common colorectal cancer consortia. *NPJ Biofilms and Microbiomes* 2017; 3:34–34. <https://doi.org/10.1038/s41522-017-0040-3> PMID: 29214046
134. Zijngel V, Leeuwen MBM van, Degener JE, Abbas F, Thurnheer T, Gmür R, et al. Oral Biofilm Architecture on Natural Teeth. *PLOS ONE* 2010; 5:e9321. <https://doi.org/10.1371/journal.pone.0009321> PMID: 20195365
135. Flemer B, Warren RD, Barrett MP, Cisek K, Das A, Jeffery IB, et al. The oral microbiota in colorectal cancer is distinctive and predictive. *Gut* 2018; 67:1454–63. <https://doi.org/10.1136/gutjnl-2017-314814> PMID: 28988196
136. Cieplik F, Zaura E, Brandt BW, Buijs MJ, Buchalla W, Crielaard W, et al. Microcosm biofilms cultured from different oral niches in periodontitis patients. *J Oral Microbiol* 2018; 11:1551596. <https://doi.org/10.1080/20022727.2018.1551596> PMID: 30598734
137. Shi H, Shi Q, Grodner B, Lenz JS, Zipfel WR, Brito IL, et al. Highly multiplexed spatial mapping of microbial communities. *Nature* 2020; 588:676–81. <https://doi.org/10.1038/s41586-020-2983-4> PMID: 33268897
138. Lötstedt B, Stražar M, Xavier R, Regev A, Vickovic S. Spatial host-microbiome sequencing 2022:2022.07.18.500470. <https://doi.org/10.1101/2022.07.18.500470>.
139. Piñero J, Queralt-Rosinach N, Bravo À, Deu-Pons J, Bauer-Mehren A, Baron M, et al. DisGeNET: a discovery platform for the dynamical exploration of human diseases and their genes. *Database (Oxford)* 2015; 2015:bav028. <https://doi.org/10.1093/database/bav028> PMID: 25877637
140. Chen EY, Tan CM, Kou Y, Duan Q, Wang Z, Meirelles GV, et al. Enrichr: interactive and collaborative HTML5 gene list enrichment analysis tool. *BMC Bioinformatics* 2013; 14:128. <https://doi.org/10.1186/1471-2105-14-128> PMID: 23586463